

# High Performance SWIR Imaging Cameras

## Introduction to SWIR Imaging

Silicon based area detectors (e.g. CCDs or CMOS) are widely used in high performance imaging applications, detecting wavelengths from soft x-ray through to near infrared (NIR). Typically the quantum efficiency (QE) of these detectors decreases rapidly as the detection wavelength increases further into the NIR region.

Detector Material		Typical VIS-IR Detection Range
Si	Silicon	400nm – 1.0µm
InGaAs	Indium Gallium Arsenide	400nm – 2.6µm
Ge	Germanium	800nm – 1.8µm
InSb	Indium Antimonide	1µm - 5µm
HgCdTe (or MCT)	Mercury Cadmium Telluride	1.5µm - 12µm

**Table 1:** Common detector materials and their typical detection range within the VIS-IR wavelength regions.

Above 1100nm, Silicon is transparent and therefore cannot be used to detect photons of these wavelengths, however many other materials do have photon sensitivity at these wavelengths and longer, see Table 1. The materials listed have been developed into detection systems which enable images to be acquired within the various regions of the visible to infrared spectrum. The typical definition for each ‘sub-region’ within VIS-IR wavelength range is outlined in Figure 1. Each of the materials above present their own advantages and challenges and therefore prior to detector selection the user must consider all aspects of the intended application, in addition to simply the wavelength response.



**Figure 1:** The typical definition of the various sub-regions of the electromagnetic spectrum, covering visible through to infrared wavelengths.

The use of imaging systems to capture long wavelength photons (beyond the detection range of Silicon based devices) continues to increase in many diverse application areas, such as life sciences, security & surveillance, non-destructive testing, quality control and astronomy. This paper will be restricted to a discussion of the performance of InGaAs detector arrays, sensitive in the VIS-SWIR region, i.e. (400 – 1700) nm.

## Brief Overview of InGaAs Detector Arrays

### Detector Construction

InGaAs is a semiconductor material which is an alloy of Indium Arsenide (InAs) and Gallium Arsenide (GaAs). Detector arrays are produced by growing an epitaxial layer of InGaAs on an Indium Phosphide (InP) substrate, with a thin passivation layer of InP grown on top of the InGaAs. The doped substrate and InGaAs layer are used to construct a photodiode array (PDA) which delivers photosensitivity, typically for wavelengths between (900 – 1700) nm. The photodiode array is then Indium bump-bonded to a CMOS ROIC (ReadOut Integrated Circuit), see Figure 2, which is used to perform the charge to voltage conversion, A/D conversion and transfer of data from the sensor.

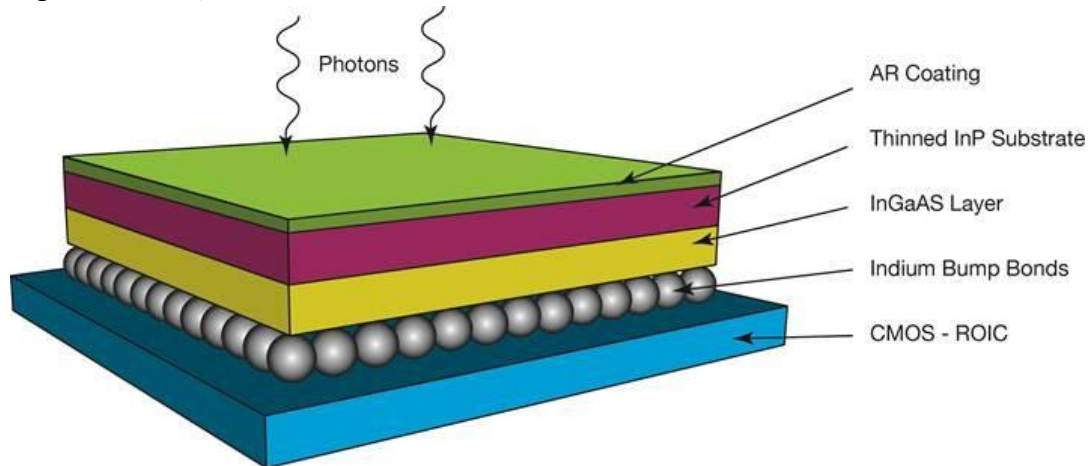


**Figure 2:** Schematic representation of the main components used in the construction of a VIS-SWIR InGaAs detector array.

This hybrid sensor fabrication results in the PDA being illuminated through the substrate layer, as illustrated in Figure 2. The InP substrate layer can prevent wavelengths below  $\approx 900\text{nm}$  from reaching the InGaAs layer, explaining the lack of visible response observed on many InGaAs detectors. However the sensors used in the Ninnox camera have the bulk of this substrate layer removed (i.e. thinned away), producing a detector with response across visible, NIR and SWIR regions. A broadband AR coating is also applied to the thinned PDA, producing a detector array which has excellent QE across the SWIR and NIR regions and good QE extending into the visible region, see Figure 3.

The long wavelength cut-off is due to the InGaAs material and can be extended (out to as far as  $2.6\mu\text{m}$ ) by increasing the fraction of InAs within the alloy; however the data presented within this paper was acquired using a sensor with a long wavelength cut-off of  $\approx 1.7\mu\text{m}$ , as per QE plot in Figure 3.

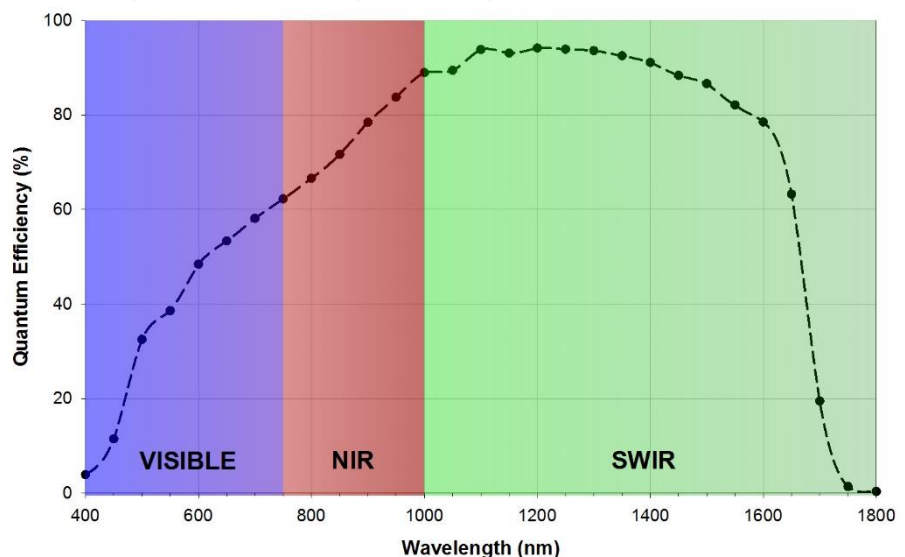


**Figure 3:** Typical QE curve for a thinned, AR-coated, VIS-SWIR InGaAs detector array, as used in the Ninnox camera.

## Detector Performance

The inherent complexity of manufacturing this type of imaging device limits the pixel sizes available to relatively large dimensions, typically  $>10\mu\text{m}$  and can result in both low manufacturing yields and the presence of defective / non-operational pixels within the final device. Available array sizes are small, when compared to CCDs / CMOS imaging devices, the largest, widely-available array size is currently  $640 \times 512$  pixels. The manufacturing complexity associated with producing a high performance InGaAs FPA, translates directly to a significantly higher sensor unit cost when compared to a Si-based detector of the same array size.

The use of a high performance CMOS ROIC delivers some advantages and disadvantages, analogous to those found on conventional Si CMOS imagers, e.g. high frame rates are achievable, short exposure times down to  $1\mu\text{s}$  can be realized and global shutter (snapshot) operation is implemented on the sensor used within the Ninnox camera. However Non-Uniformity Corrections (NUCs) must be applied in order to reduce fixed pattern noise (FPN) introduced by the CMOS ROIC. The application of NUCs is software selectable on the Ninnox camera, as is the defective pixel replacement feature.

In addition to the increased sensor costs and FPN, the two main disadvantages associated with InGaAs detector arrays have been high readout noise and high dark current.

## Readout Noise

The readout noise is strongly influenced by the quality / performance of the CMOS ROIC integrated within the detector. Historically ROIC designs provided typical readout noise levels in the range 200 – 700 electrons, depending upon the amount of gain applied. This is acceptable for use in thermal imagers and the detection of 'bright' signals, provided there is sufficient pixel well depth to store signals large enough to overcome the high noise floor and provide an acceptable signal to noise ratio.

However low light detection was not possible and the intra-scene dynamic range was limited. The latest generation of ROIC design has been utilized in the Ninnox camera and enables data to be readout via one of two gain modes:

- i. High Gain (HG) Mode – offering the lowest readout noise ( $<50e^-$ ) but with limited pixel well depth ( $>10ke^-$  pixel)
- ii. Low Gain (LG) Mode – for maximum dynamic range, offering the maximum pixel well depth ( $>650ke^-$  per pixel) but with increased readout noise ( $<195e^-$ ). This provides an intra-scene dynamic range  $>70\text{dB}$ .

## Dark Current

The small bandgap of InGaAs ( $\approx 0.75\text{eV}$  at room temperature) means that it is much easier to thermally promote electrons from the valence band into the conduction band, compared to silicon for example. This manifests as a significantly higher dark current in InGaAs detectors, when compared to silicon based detectors with similar pixel sizes. Some early generation devices suffered from dark currents of the order  $10^6 e^-/\text{pix}/\text{sec}$  ( $\approx 160\text{fA}/\text{pix}$ ) at room temperature ( $+25^\circ\text{C}$ ), approximately four orders of magnitude higher than pinned silicon-based detectors. Obviously this level of dark current severely limits the range of exposure times that could be used for image acquisition, as dark signal and its associated shot noise rapidly became the dominant features in acquired images. Detector manufacture has improved, reducing dark current to the order of  $\approx 10^3 e^-/\text{pix}/\text{sec}$  ( $\approx 16\text{fA}/\text{pix}$ ) at room temperature. The Ninnox camera utilizes Raptor Photonics Pentavac™ technology and actively cools the InGaAs FPA in order to reduce the dark current to approximately  $10^3 e^-/\text{pix}/\text{sec}$  ( $0.16\text{fA}/\text{pix}$ ). This is achieved using only moderate cooling power, attaining a detector temperature of  $\approx -20^\circ\text{C}$ , thus minimizing the shift in the long wavelength response cut-off and maintaining a compact camera form factor. (The shift in the long wavelength cut-off is due to the temperature dependence of the InGaAs bandgap energy – the bandgap increases slightly as the material temperature decreases).

Inferior ROIC architectures and designs can necessitate deeper cooling of the sensor to achieve comparable dark current performance. These cryogenic / deep-cooled camera systems are typically physically much larger in size, significantly more expensive and result in much larger shifts in the long wavelength response cut-off.

The final camera performance is determined by a combination of the quality of the InGaAs PDA and the performance of the CMOS ROIC, in addition to the design and implementation of the camera electronics and firmware. The Ninox camera has optimized all these components to deliver the best scientific performance available from a VIS-SWIR imaging camera, as detailed in the following sections.

## Dark Current (and Dark Noise) Reduction

Cooling the InGaAs FPA provides a dramatic decrease in the measured dark current per pixel, as shown in Figure 4 below. The calculated dark current doubling temperature is approximately 7°C, which is similar to the dark current temperature dependence observed on Silicon based FPAs.

The diverse range of applications for which VIS-SWIR image detectors can be used place a variety of requirements on the camera / imaging system, including the use of different gain modes, frame rates and exposure times.

Some applications may require little or no cooling in order to deliver the required performance, however some more demanding applications may benefit from cooling the InGaAs FPA to temperatures 40°C or 50°C below the ambient, in order to reduce dark current shot noise and increase the accessible dynamic range.

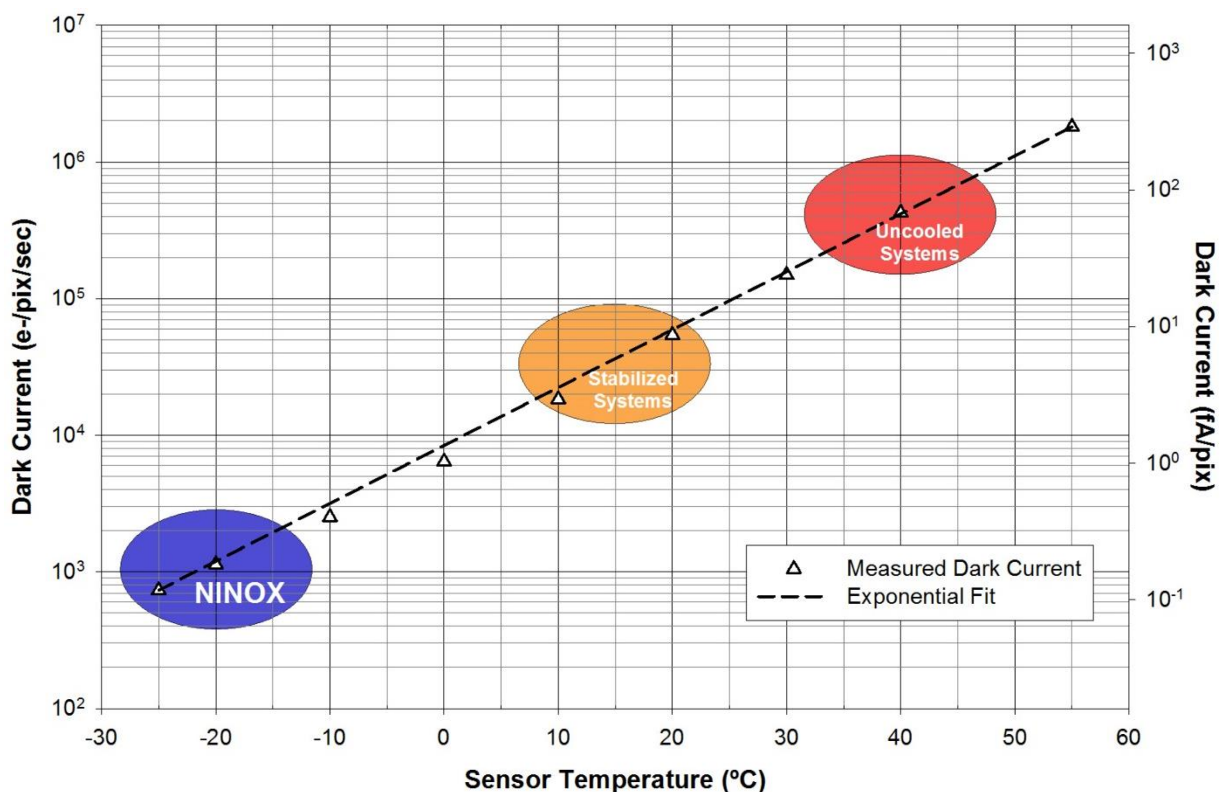


**Figure 4:** Typical variation of measured dark current with temperature for the InGaAs FPA used within the Ninox camera.

Uncooled systems typically operate with sensor temperatures around +40°C, whereas stabilized systems operate with sensor temperature typically close to +15°C. The Ninox camera employs thermoelectric cooling inside a PentaVac™ vacuum enclosure to provide a compact and maintenance-free method of cooling the sensor to temperatures of ≤-20°C.

As can be seen from Figure 4, the cooling performance offered by the Ninox camera translates to a dark current reduction of more than one order of magnitude, when compared to a stabilized system and more than two orders of magnitude, compared to an uncooled system.

The effect of dark current on the image can be visualized by comparing dark frames of equal exposure time, acquired at different sensor temperatures, as shown in Figure 5. The high dark current is clearly visible as speckle in the 10 second dark frame acquired at +20°C. Plotting a horizontal cross section (in the above case through the centre of the image) helps to visualize the impact the dark current and associated shot noise will have on any image acquired under these conditions. The presence of relatively high pixel values in this dark frame indicate that a significant fraction of the pixel full well capacity is being wasted, as it is storing dark signal as opposed to any signal the user is attempting to capture.

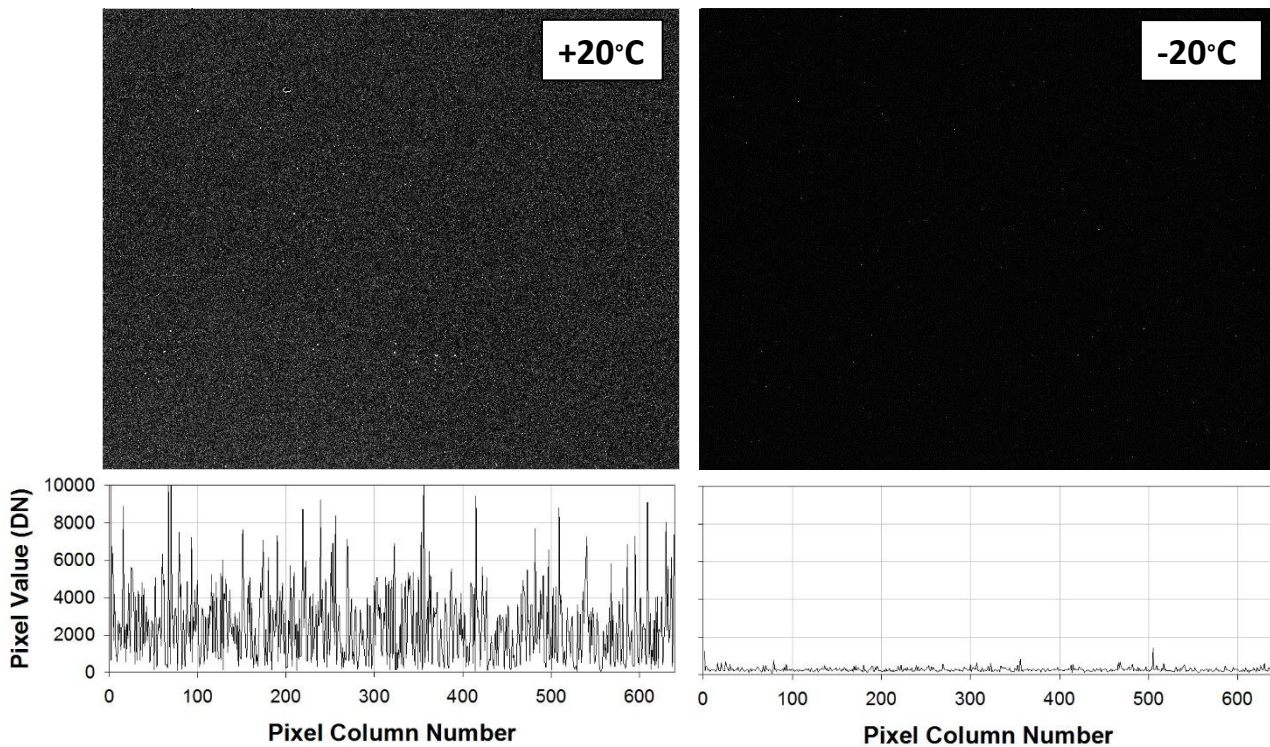


**Figure 5:** 10 second dark frames acquired at sensor temperatures of +20°C and -20°C. Note the same grayscale is used for both images. The line plots are horizontal cross sections along the central row of each image.

The spikey nature of the image, indicative of a raised noise, in this case due to dark current shot noise, will degrade the final image quality as any detected signal will be superimposed upon this noise floor. The combination of these two effects, reduced useable full well capacity and increased noise floor, will severely limit the maximum signal to noise ratio which can be achieved under these operating conditions. However assessing the 10 second image which was acquired at a sensor temperature of -20°C, it is evident that relatively little of the pixel well capacity has been consumed by dark current and also the noise floor is dramatically lower as a result of the reduction in dark current.

An alternative means of assessing the impact of cooling the sensor is to compare histograms of dark frames, for a device at two different test temperatures. Figure 6 compares histograms of 100ms exposures taken at sensor temperatures of +20°C and -20°C (in high gain mode). The impact of dark current is clearly visible as the peak pixel occurrence shifts to a higher value at the warmer sensor temperature. Not only does this dark current introduce a higher dark current shot noise component, but it also partially fills the wells of the pixels, which prevents this portion from being used to capture

image data by the user. So it is clear that these effects will be detrimental to both the signal to noise ratio and the accessible dynamic range of the detector system.

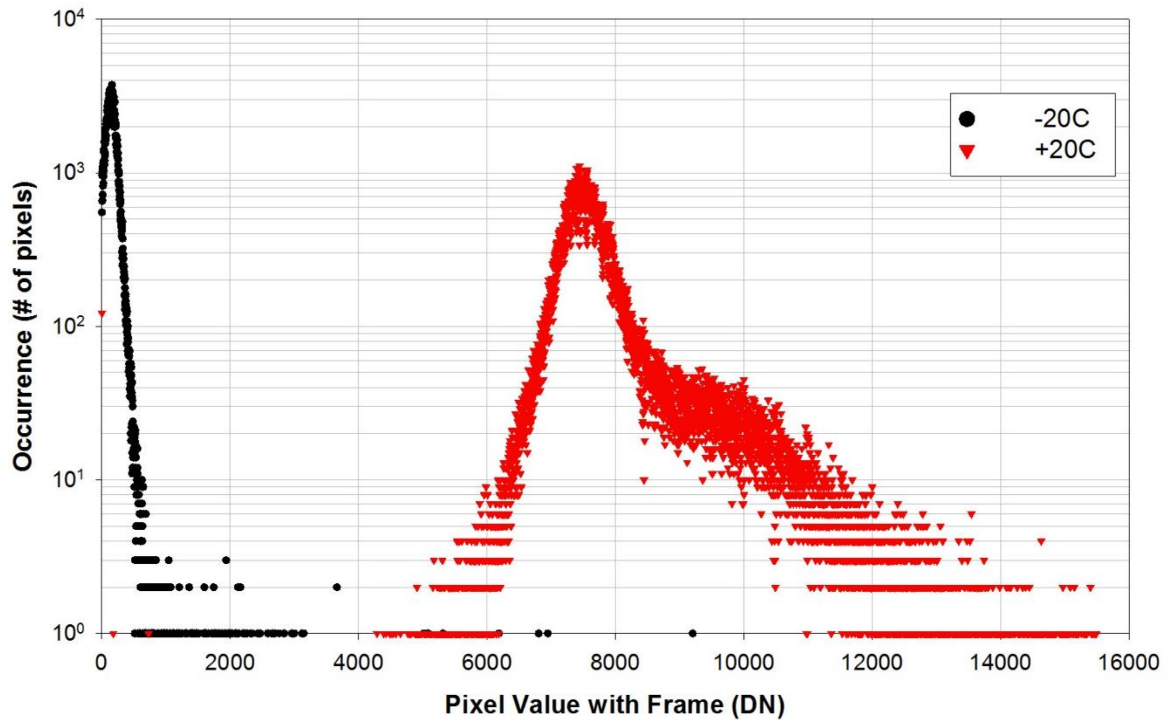


Figure 6: Histogram plots of 100ms dark frames taken at two different sensor temperatures in high gain mode.

Using typical values for sensor read noise and dark current, it is possible to estimate the theoretical ‘accessible dynamic range’, which we define as follows:

$$\begin{aligned}
 \text{Accessible Dynamic Range} &= \frac{\text{Accessible Pixel Well Depth}}{\text{Dark Noise}} \\
 &= \frac{\text{Accessible Pixel Well Depth}}{(\text{Read Noise}^2 + \text{Dark Shot Noise}^2)^{1/2}} \\
 &= \frac{\text{Accessible Pixel Well Depth}}{(\text{Read Noise}^2 + \text{Dark Signal})^{1/2}} \\
 &= \frac{\text{Pixel Full Well Capacity} - (\text{Mean Dark Current} \times \text{Exposure Time})}{(\text{Read Noise}^2 + \text{Dark Signal})^{1/2}}
 \end{aligned}$$

Producing a plot of this accessible dynamic range as a function of exposure time can indicate to the user the parameter space over which the camera will serve as a useful detector, delivering a specific dynamic range. Examples of these plots are shown below in Figure 7, which show the typical operation of the Ninox camera, operating with a sensor temperature of -20°C compared to the same sensor operating at a temperature of +20°C.

The graph clearly shows the benefit of cooling the InGaAs FPA as the accessible dynamic range for both gain modes are preserved for longer exposures, up to several seconds for the high gain mode and up to several hundred seconds for the low gain mode.

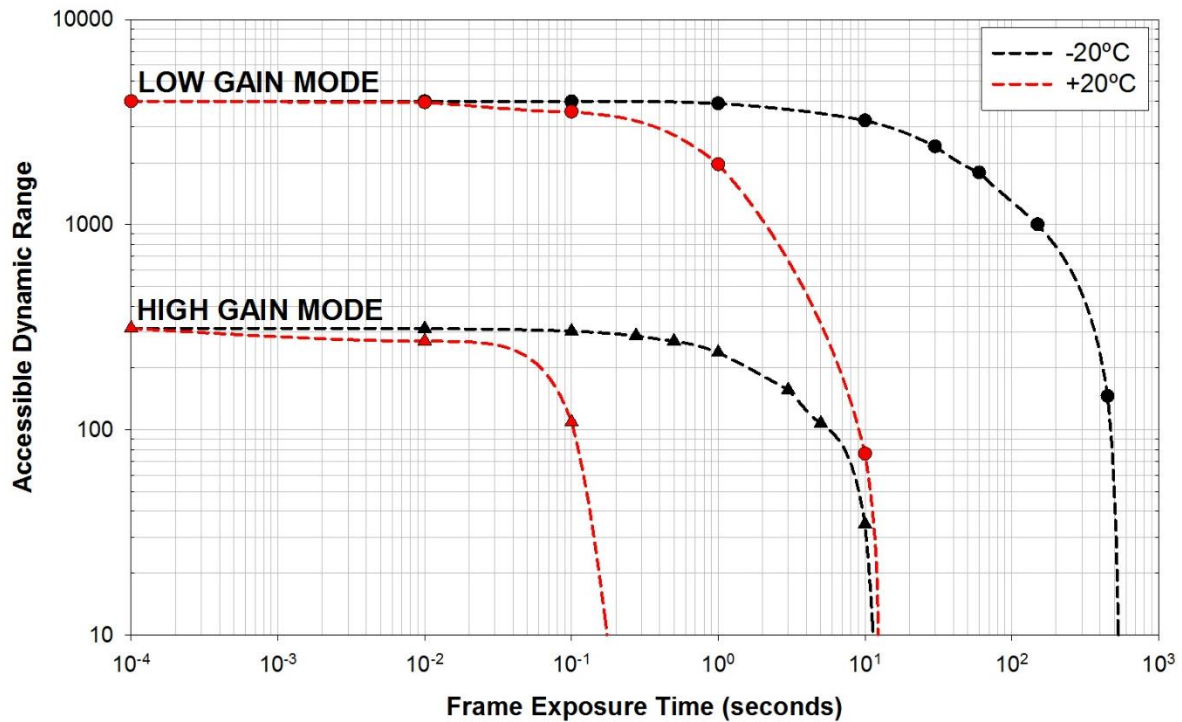


**Figure 7:** Plots of 'Accessible Dynamic Range' versus exposure time for the Ninnox InGaAs FPA at two different temperatures. Low gain mode maximizes dynamic range whereas high gain mode minimizes readout noise.

## Photon Transfer Curve and Linearity

Constructing a photon transfer curve for the camera allows the users to quantify the performance of the camera. Variance photon transfer curves have been constructed for Ninnox cameras at a sensor temperature of -20C. Using the calculated conversion factors, the measured data can be converted from arbitrary units, i.e. Digital Numbers (or DN) into absolute units, i.e. electrons. Figure 8 shows a typical plot acquired on a Ninnox camera, with the circular points showing the actual measured total noise as a function of mean signal level.

Further analysis of the data shows that the dark noise floor (due to readout noise and any dark current shot noise) is just over 150 electrons in this configuration (Low gain mode, sensor temperature = -20°C and exposure time 300ms) and the full well capacity is just under 600ke-/pixel on this device. Deconvolving the dark noise component from the total measured noise, should leave data which displays an ideal shot noise limited dependence, i.e. noise equal to the square root of the signal, indicated by the dashed line in Figure 8.

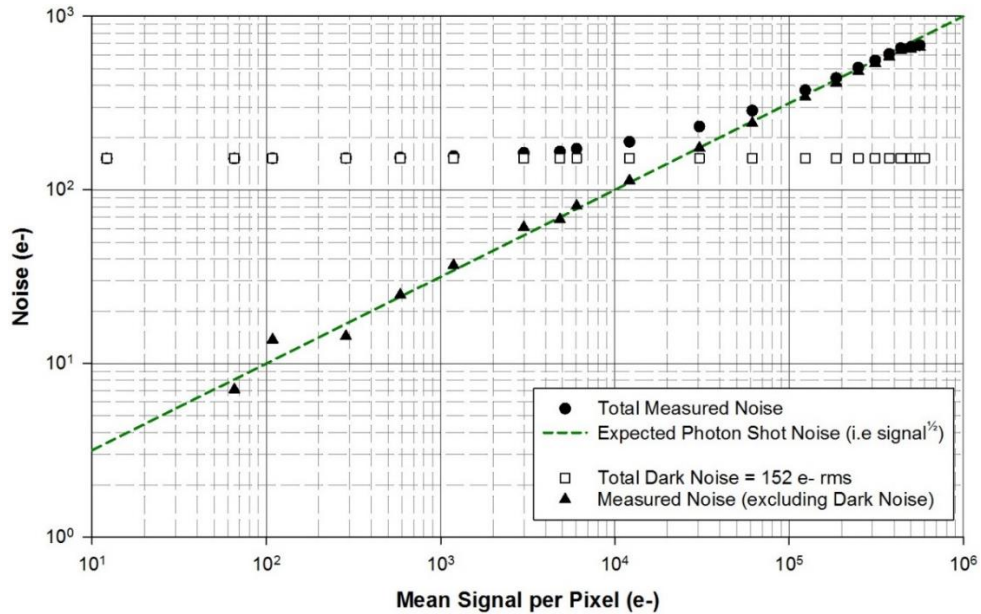


**Figure 8:** Sample Photon Transfer Plot for Ninox camera, acquired in low gain mode with the sensor cooled to  $-20^{\circ}\text{C}$  and an exposure time of 300ms. Excellent agreement between measured and theoretical shot noise performance across the entire range of measured signals.

As can be seen from the graph there is excellent agreement between the theoretical line and the experimental data (triangular points) across the entire range of measured signal (approximately 100 – 600 000 electrons per pixel). The linearity performance of the Ninox camera is illustrated in Figure 9. This analysis also shows the expected agreement between measured data and a straight-line fit with a non-linearity of  $<0.7\%$  calculated across the measured signal range.

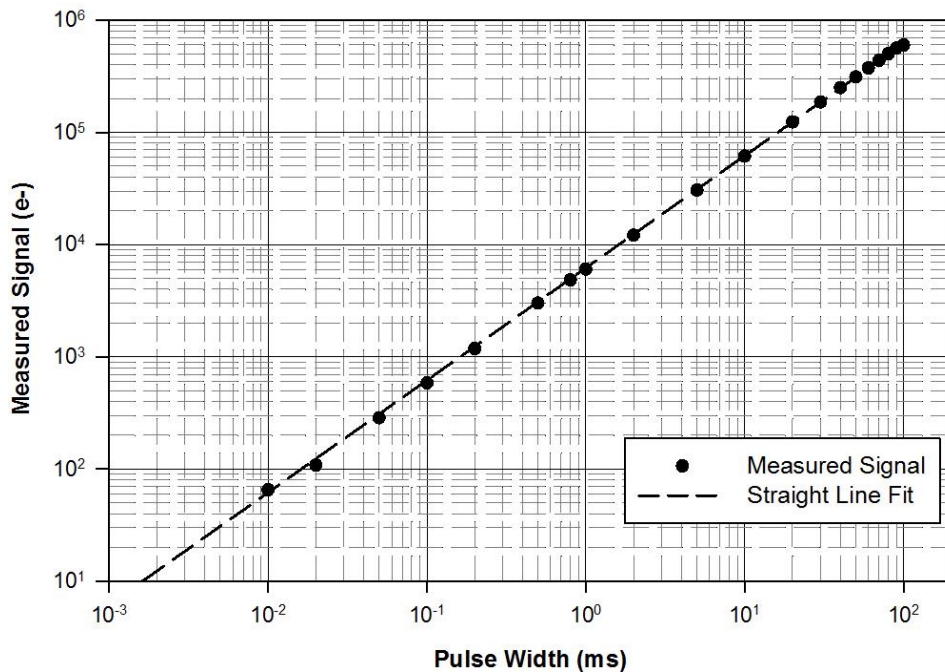


**Figure 9:** Linearity plot for Ninox camera, acquired in low gain mode with the sensor cooled to  $-20^{\circ}\text{C}$  and an exposure time of 300ms. Signal level was varied by changing the pulse width of the light source. Excellent agreement is observed between measured data and a straight-line fit, with the non-linearity being determined to be  $<0.7\%$ .



## Sample Application Images

The improvement in sensitivity and dynamic range made possible by the latest generation, moderately cooled SWIR camera, opens a range of new observation possibilities. Astronomy is just one application which can leverage the high performance of the Ninox camera, as many observations are recorded within the J band, wavelengths = (1.1 - 1.4)  $\mu\text{m}$  and the H band, wavelengths = (1.5 to 1.8)  $\mu\text{m}$ .

### Orion Nebula, Visible vs SWIR imaging

The Orion nebula is a textbook example of what SWIR astronomy can reveal. The centre of the nebula consists of a very dense dust cloud masking the stars being born in its centre.

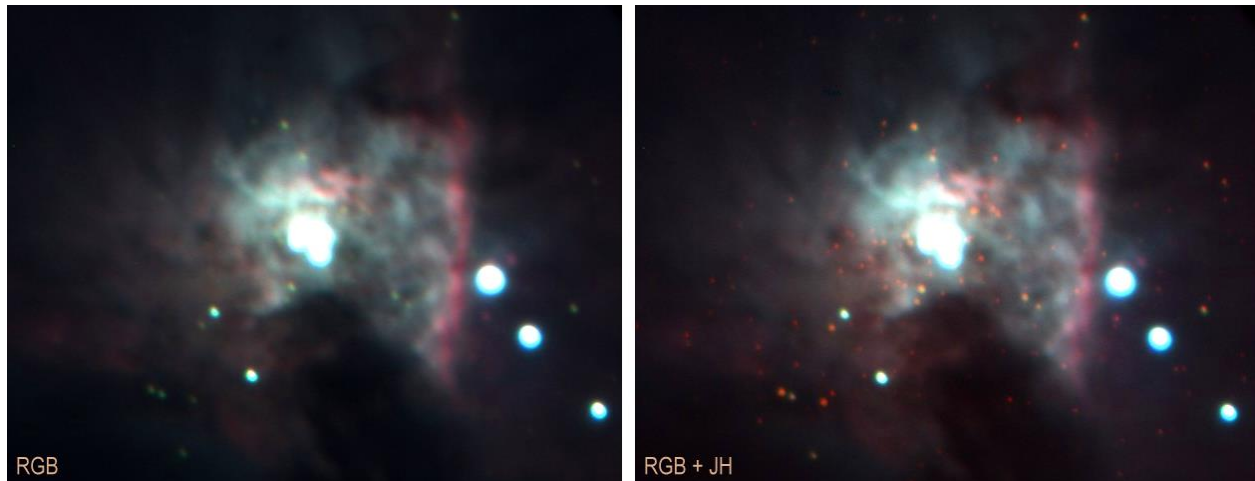


**Figure 10:** Orion Nebula in visible (left) visible and J and H band (right). Courtesy of Alain Klotz<sup>1</sup>

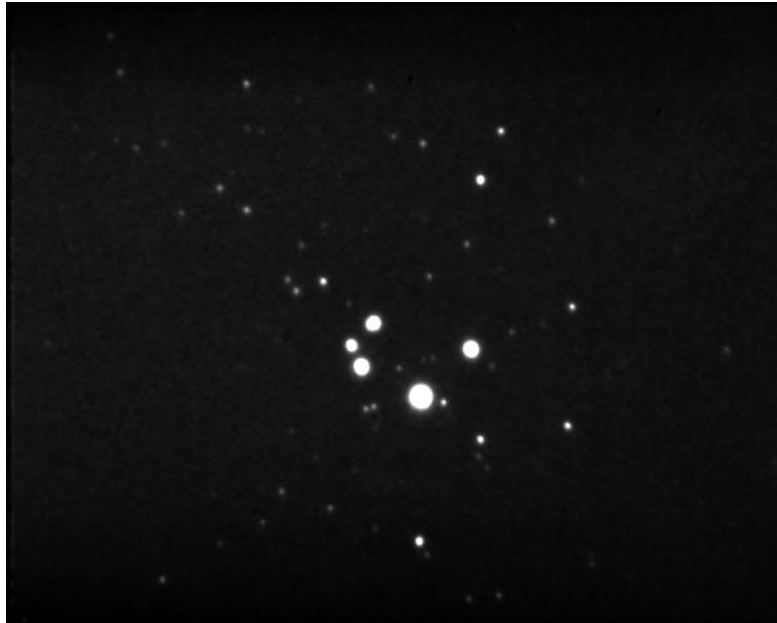
Standard visible imaging, on the left, is enhanced by the SWIR image in orange on the right. The SWIR image was obtained combining 9 exposures of 2sec in High Gain of a moderately cooled InGaAs-FPA camera and would have been impossible to obtain with a standard, temperature stabilized SWIR camera. Notice how the central stars, hidden in the visible image, are clearly evident in the SWIR image.

Figure 11 represents the core of the Trapezium cluster in the heart of the Orion nebulae, observed in the astronomical H band (1.625 $\mu\text{m}$ ) at the Cassegrain focus of the 1 meter Omicron telescope of the C2PU facility (Observatoire de la Côte d'Azur).

This region of the sky contains many young stars which formed in that dust-rich environment. Stellar components of this open cluster are better observed at infrared wavelengths because of the lower absorption of the dust.

The faintest stars are about H=13 magnitude. The final image is composed of a stack of 4000 shift-and-added, 15ms exposure frames.

<sup>1</sup>Alain Klotz, IRAP France, aklotz@irap.omp.eu



**Figure 11:** Core of the trapezium cluster in the heart of the Orion nebula, H band. Courtesy of Lyu Abe<sup>2</sup>

#### Uranus, SWIR imaging

Figure 12 shows an image of Uranus observed in the astronomical H band (1.625 $\mu$ m) at the Cassegrain focus of the 1 meter Omicron telescope of the C2PU facility (Observatoire de la Côte d'Azur). The planet is about 20 times farther away from the sun than Earth. Its apparent diameter on this image is about 2.9 degrees.

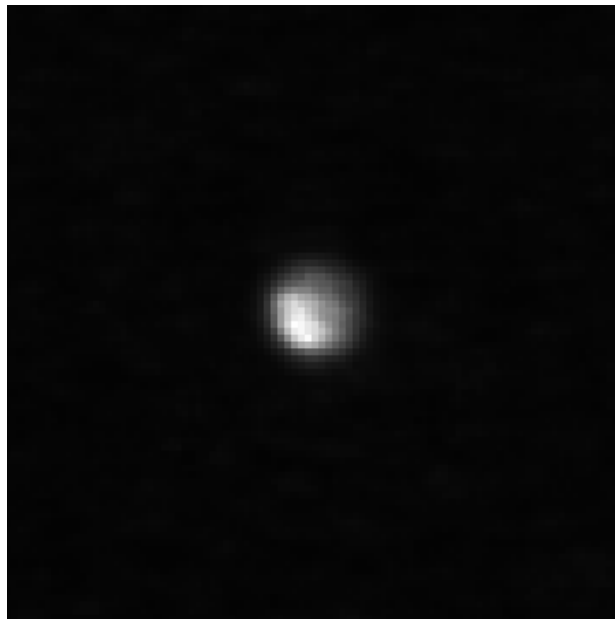


**Figure 12:** Uranus observed in the astronomical H band. Courtesy of Lyu Abe<sup>2</sup>

The observed surface inhomogeneity is caused by clouds in the atmosphere of Uranus. The final image is composed of a stack of 1000 shift-and-added, 51ms exposure frames.

---

<sup>2</sup>Lyu Abe, Laboratoire Lagrange, UMR 7293, Lyu.Abe@unice.fr

## Summary

Standard characterization techniques have been used to quantify the performance of a moderately cooled InGaAs FPA within the Ninnox camera. The intra-scene dynamic range has been verified to be high (>70dB) with excellent linearity. Low noise performance is achieved through both high and low gain readout modes.

Cooling the FPA to a temperature of -20°C significantly reduces the dark signal and associated noise within images, enabling acquisition of quantitative data with exposure times of up to several minutes. The improvement in image quality, as a result of this cooling, has been illustrated and some sample images from a range of applications are presented.

Pentavac™ technology enables moderate cooling of the InGaAs FPA using minimal input power. The shift in the long wavelength response cut-off is reduced, compared to cryogenically / deep-cooled systems, and therefore the Ninnox camera offers superior performance in an affordable, rugged, compact form factor.

## About Raptor

Raptor has spent many years developing both SWIR and VIS-SWIR technology into some of the highest performing cameras available today.

Raptor also offers a range of other cameras using silicon based sensors including CMOS, CCD and EMCCD. Visit our web-site for more information.

## Author Profile

Dr. Geoff Martin is Principal Systems Engineer at Raptor Photonics Ltd, based in Northern Ireland. Raptor is a leading developer of high performance digital cameras using CCD, EMCCD, sCMOS and InGaAs detector arrays. The selection of sensor type, required cooling performance and cooling method can be discussed with Raptor Photonics team to identify the ideal solution for your application.

For more information contact Raptor Photonics Ltd as follows:

[sales@raptorphotonics.com](mailto:sales@raptorphotonics.com) or Tel: +44 2828 270 141

### D-A-CH

Laser 2000 GmbH  
82234 Wessling  
Tel. +49 8153 405-0  
info@laser2000.de  
www.laser2000.de

### FRANCE – Telecom

Laser 2000 SAS  
78860 St-N. I. Bretèche  
Tel. +33 1 30 80 00 60  
info@laser2000.fr  
www.laser2000.fr

### FRANCE – Photonic

Laser 2000 SAS  
33600 Pessac  
Tel. +33 5 57 10 92 80  
info@laser2000.fr  
www.laser2000.fr

### IBERIA

Laser 2000 SAS  
28034 Madrid  
Tel. +34 617 308 236  
info@laser2000.es  
www.laser2000.es

### NORDICS

Laser 2000 GmbH  
112 51 Stockholm  
Tel. +46 8 555 36 235  
info@laser2000.se  
www.laser2000.se